Electronic Supporting Information

to: Unspecific ligand binding yielding stable colloidal ITO-nanoparticle dispersions

by C. Grote, K. J. Chiad, D. Vollmer, and G. Garnweitner

A. Experimental Details

The ITO nanoparticles were synthesised according to the nonaqueous synthesis in benzyl alcohol as described earlier.[S1] Nanoparticles with 15 wt.-% SnO_2 were utilised for all presented stabilisation experiments. The obtained turbid dispersions were centrifuged (4650 g for 10 min) and the precipitates resuspended in the same volume of chloroform (anhydrous, 99+%, Aldrich). After another centifugation treatment, the precipitates were redispersed in the desired solvent ($CHCl_3$ anhydrous, 99+% or water, de-ionised, 0.06 µS cm^{-1}) and used as obtained for all treatments and analyses.

B. Characterisation of ITO nanoparticle dispersions

The NMR measurements were carried out on a Bruker AV II-300 device. The reaction mixtures were characterized by ^1H NMR (300 MHz, $CDCl_3$, TMS) measurements.

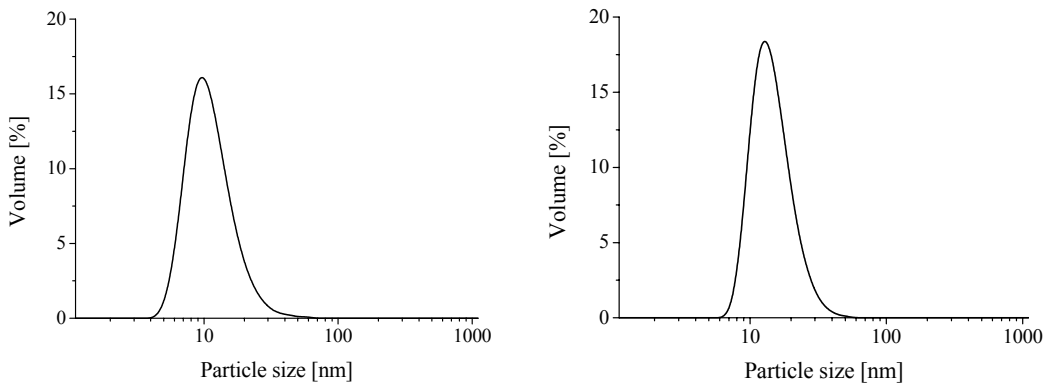

Fig S1. Size distribution by volume for stabilised ITO-nanoparticles in $CHCl_3$ using dodecylamine as stabiliser (left) and for stabilised ITO-nanoparticles in aqueous dispersion using propylamine (right) (recorded on a Malvern Zetasizer Nano ZS instrument under a detector position at 173 °, backscatter detection). No changes in the particle size distributions were observed for repeated measurements on dispersions after 1, 2, 3, and 6 months storage in closed vials at room temperature.

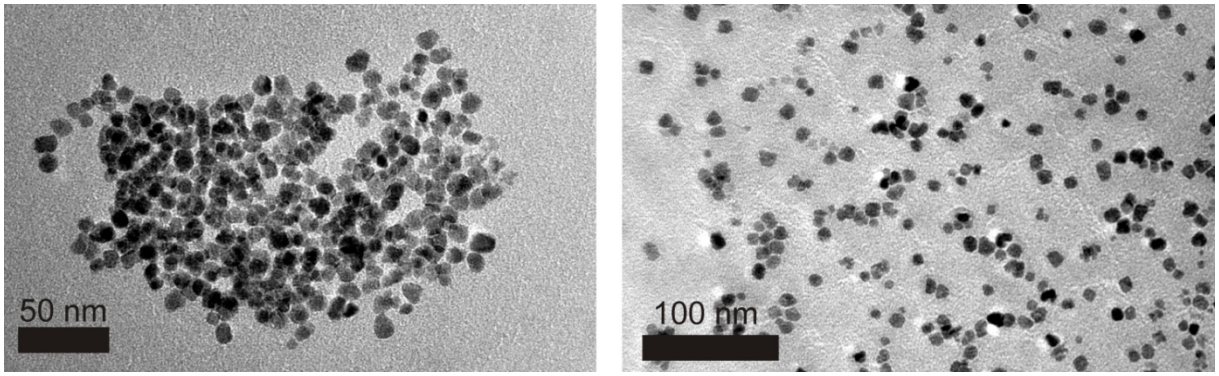

Fig S2. TEM images of unstabilised ITO-nanoparticles (left) and stabilised (with dodecylamine) ITO-nanoparticles (right), recorded on a JEOL JEM-2100 at 100 kV.

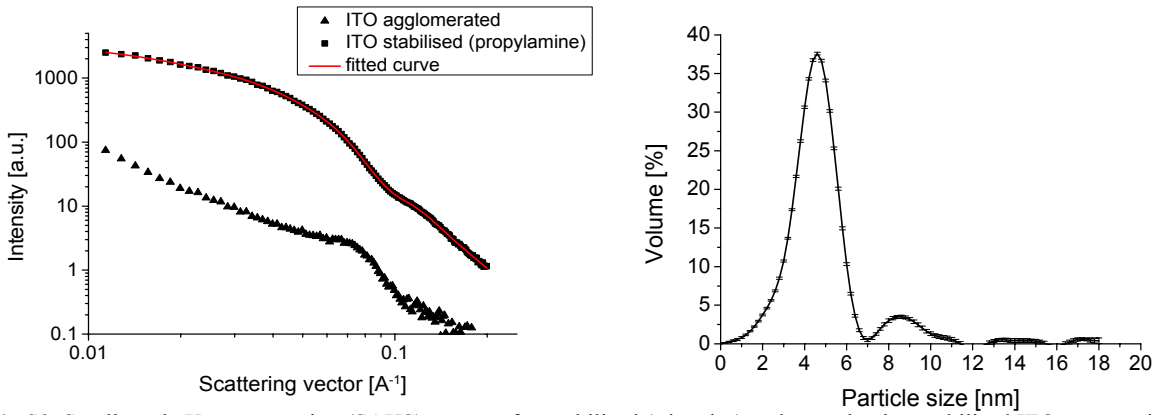

Fig S3. Small-angle X-ray scattering (SAXS) curves of unstabilised (triangles) and propylamine-stabilised ITO nanoparticles in aqueous dispersion (left); size distribution derived from the fitted curve for the stabilised dispersion (right); determined on a NanoSTAR SAXS system (Bruker AXS GmbH, Karlsruhe, Germany).

The ITO-nanoparticle dispersions were analysed by DLS and SAXS. Due to the strong X-ray absorption of $CHCl_3$, however, only the aqueous dispersions could be utilised to perform SAXS investigations. The scattering curves show strong differences between the two samples, with the generally lower scattering intensity of the unstabilised sample attributable to fast sedimentation in the agglomerated sample. For the stabilised sample, also a size distribution could be calculated from the SAXS curve by obtaining a fitting procedure (GNOM software, EMBL Hamburg).[S2] The obtained particle size distribution (Fig. S3 (right)) is much more well-resolved than the DLS-derived data and slightly below those obtained by DLS, as latter measures the hydrodynamic radius, which always exceeds the hard core radius. Both methods however clearly prove that essentially only primary particles are present in the dispersions. The stabilisation effect can also be traced on the TEM images (Fig. S2). The small number of agglomerates visible in the micrograph of stabilised particles is attributed to drying effects during sample preparation.

C. Isothermal titration calorimetry (ITC) analysis

To quantify the binding affinity of alkylamines to the surface we applied isothermal titration calorimetry (VP-ITC, Microcal Inc., USA), a technique intensively used to characterise biomolecular interactions.[S3]

The ITC device consists of two cells, a sample cell and a reference cell, 1.4 ml each. To carry out a binding experiment, the sample cell was loaded with an ITO/$CHCl_3$ dispersion (5 mM ITO in $CHCl_3$; anhydrous $CHCl_3$, 99+%, was used for all ITC experiments), and the reference cell was filled with the solvent ($CHCl_3$). A long-needle syringe (nominal volume 250 µl), with a twisted paddle fastened to its end, was filled with a solution of the ligand (benzyl alcohol, alkylamine, dopamine) dissolved in $CHCl_3$ (50 mM solution). The difference in heat that needed to be added to the reaction (sample) and reference cells to keep both cells at the same temperature was monitored over time. Each peak represents the heat change associated with the injection of 1.5 µl of the respective ligand/$CHCl_3$ solution into the nanoparticles/$CHCl_3$ dispersion. Only in case of the first injection, 0.5 µl of the respective ligand/$CHCl_3$ solution was used, to ensure identical starting conditions. This heat change was not evaluated. The quantity of released heat is proportional to the binding strength. If the reaction is exothermic, less heat needs to be added to the reaction cell and a negative heat signal is obtained. As the available binding sites on the nanoparticle surface become progressively occupied during the titration of the ligand, the heat signal decreases and eventually saturates. Finally, only heats of dilution are observed.

In order to subtract the heats of dilution due to dissolving the ligand in chloroform, dilution experiments were conducted. In these experiments a 50 mM solution of ligand dissolved in $CHCl_3$ was titrated into $CHCl_3$. The heat was subtracted from the data obtained from the titration of the ligand into the nanoparticle/$CHCl_3$ dispersion.
A binding curve was then obtained from a plot of the heats from each injection against the molar ratio of ligand to nanoparticles, equal to the number of ligand molecules per nanoparticle. This molar ratio was calculated from the average molar mass of the nanoparticles, assuming an average ITO particle diameter of 10 nm and TiO_2 particle diameter of 4 nm, spherical shape and bulk density.

The data analysis was performed using the ORIGIN 7.0 based software. The single-site binding constant K_B and the heat of binding ΔH were estimated as adjustable parameters in a fitting procedure using a nonlinear least-squares approach (Levenberg-Marquardt algorithm).[S4,S5]
The single-site binding constant is given by:[S5,S6]

$$K_B = \frac{[ML]}{[M][L]}$$

where [M] denotes the concentration of nanoparticles, [L] the concentration of ligand (benzyl alcohol, alkylamine or dopamine) and [ML] the concentration of nanoparticle–ligand complexes, i.e. M + L = ML.
The entropy ΔS and free energy ΔG of binding are given by:

$$\Delta G = -RT \ln K_B = \Delta H - T\Delta S$$

where R is the gas constant and T is the absolute temperature.

To ensure that the enthalpies and entropies were evaluated after the system attained equilibrium one titration every 5 minutes was performed. A high magnification image of the first 4 titrations is given in Fig. S4, showing that the system achieved equilibrium about three minutes after a titration. Waiting for 5 minutes between successive titrations ensured that the dispersion obtained equilibrium.

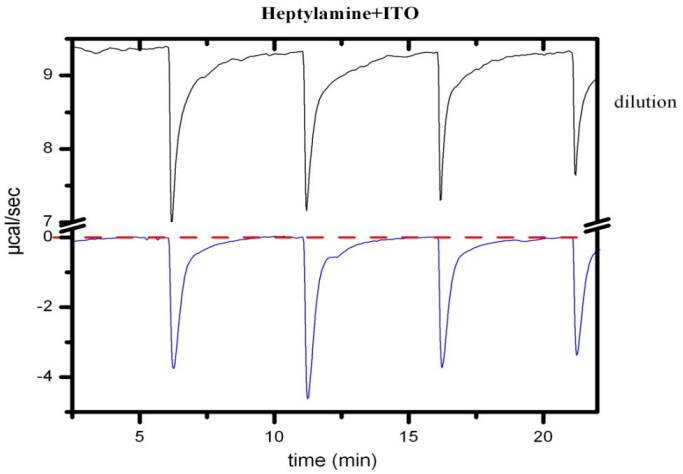

Fig S4. Magnification of the first 4 titrations, of 1.5 µl each. The upper curve shows the dilution (50 mM heptylamine dissolved in $CHCl_3$ was titrated into $CHCl_3$) and the lower curve shows the titration of 50 mM heptylamine dissolved in $CHCl_3$ to 5 mM ITO in $CHCl_3$. Three minutes after each titration the heat signal is almost constant.

Furthermore, the influence of the number of titrations was investigated, Fig. S5. The left figure shows the heat signal after 1 titration of 0.5 µl followed up by 24 titrations of 1.5 µl each. The number of titrations was doubled in case of the right titration curve, i.e. 1 titration to 0.5 µl followed by 49

titrations to 1.5 µl. Independently of the number of titrations, the change in enthalpy was almost identical. In case of 24 titrations ΔH = -14.6 ± 4 kJ and in case of 50 titrations ΔH = -15.3 ± 3.5 kJ. These results indicate that indeed the surface coverage was investigated under equilibrium conditions.

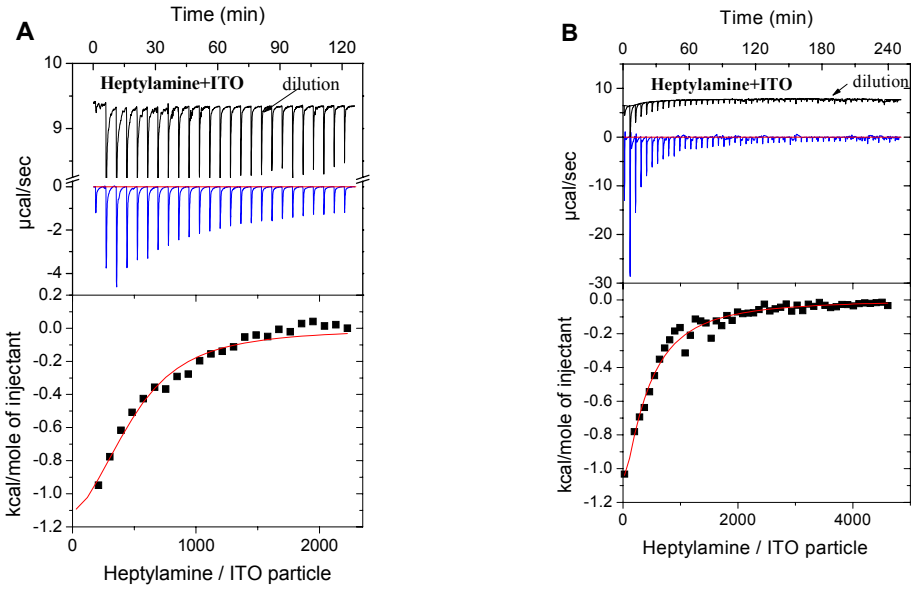

Fig S5. The influence of the number of titrations on the thermogram. A) 1 injection of 0.5 µl and 24 injections of 1.5 µl of 50 mM heptylamine in $CHCl_3$ to 5 mM ITO nanoparticles dispersed in $CHCl_3$, B) 1 injection of 0.5 µl and 49 injections of 1.5 µl of 50 mM heptylamine in $CHCl_3$ to 5 mM ITO nanoparticles dispersed in $CHCl_3$.

The shape of the ITC curves does not depend on the amine, however the absolute values do. For example, the stoichiometry factor N increases with the chain length of the amine; propylamine: N = 220 ± 40, pentylamine: N = 360 ± 55, heptylamine: N = 430 ± 100, dodecylamine: N = 550 ± 90. N denotes the inflection point of the binding isotherm and is a measure of the number of binding sites per particle, assuming an equal number of binding sites per particles. Likely, the dependence of N on the amine originates from the fact, that only a certain fraction of ITO nanoparticles can be stabilised, see Fig. 5 in the main manuscript. The maximal stabilised fraction, reached when adding a certain amount of amine, can not be increased by further increasing the amount of amine added to the dispersion. Therefore, it can not be excluded that the number of binding sites is not homogeneously distributed, i.e. ITO nanoparticles with more amines per particle coexist with particles having less amines per particle. The reason why the average number of amines per particle seems to differ is under investigation. TiO_2 nanoparticles show a higher stoichiometry factor, N = 2600 ± 700, in line with the stronger binding affinity of dopamine on TiO_2.

Fig. S6, top, shows the measured titration curves for the different systems measured under the typical conditions. The area underneath each injection peak is equal to the total heat released for that injection. In Fig. S6, bottom, the plots of the heats from each injection against the molar ratio of ligand to nanoparticles are displayed. As described above, the data points could be fitted to obtain the binding curves (solid red lines).

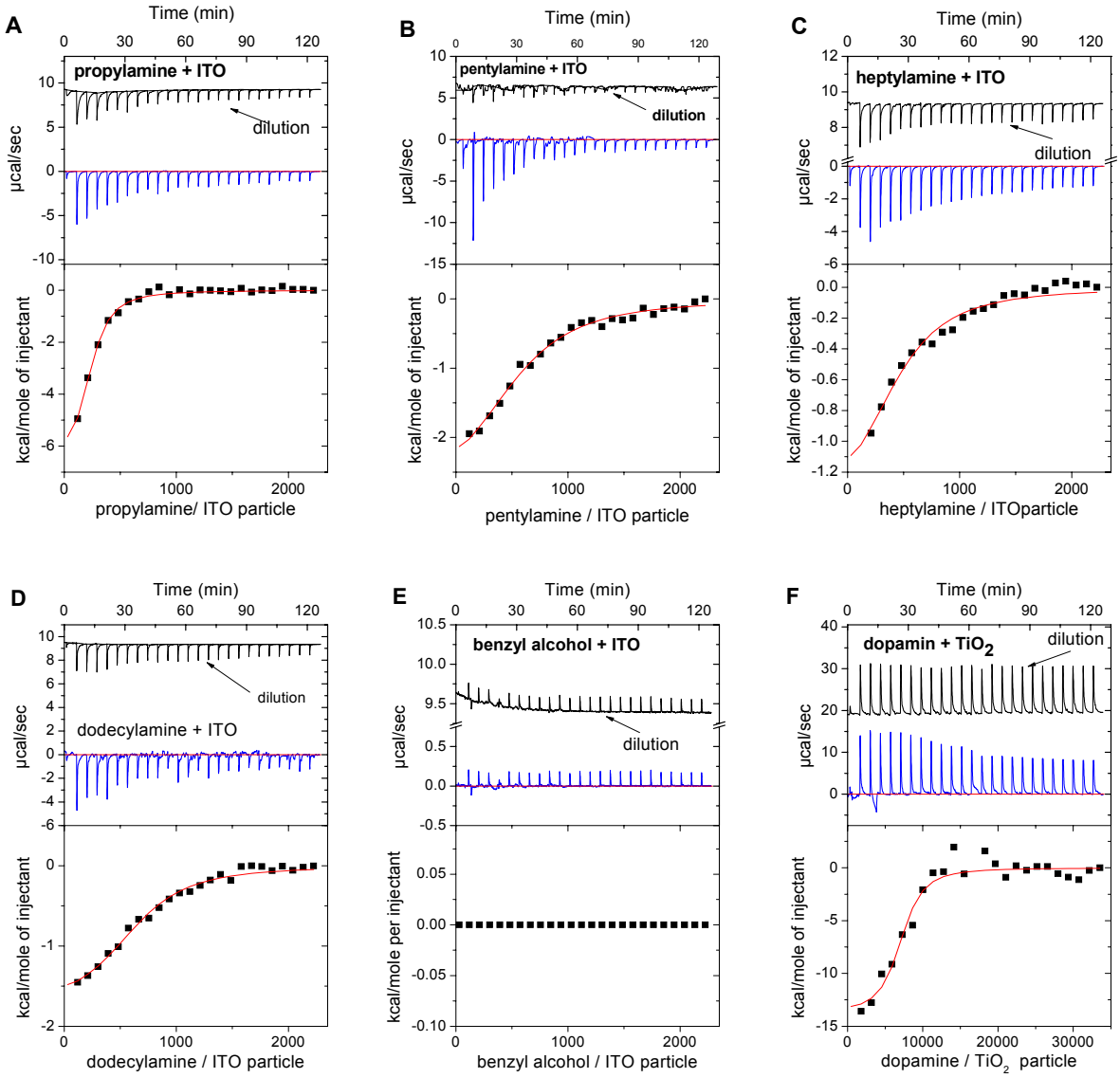

Fig. S6. Top panels**:** Twenty four injections of 1.5µl of ligand were added to the ITO dispersions (A to E), and TiO_2, respectively. A) propylamine, B) pentylamine, C) heptylamine, D) dodecylamine, E) benzyl alcohol added to ITO, and F) dopamine added to TiO_2 particles. In case of A) to D) 50 mM amine dispersed in chloroform was added to 5 mM ITO molecules dispersed in chlorofrom. E) 25 mM amine dispersed in chloroform was added to 0.05 mM TiO_2 molecules dispersed in chlorofrom. Bottom panels: This integrated heat from each injection is plotted against the molar ratio of ligand and nanoparticles. The solid red line shows the fit of the data points using a one site model.[S5,S6]

To verify that the generic behaviour of the ITC data does not depend on the concentration of amine and ITO, we investigated the dependence of the binding isotherms on different concentrations of dodecylamine and ITO in detail, Figs. S7 and S8. Whereas the shape of the curves is always the same, the absolute values vary by a factor of two, i.e. ΔH = (-17 ± 8) kJ/mol. We expect that the measurement of the heat of dilution forms the most important error source. The heat of dilution needs to be subtracted from the ITC curves to obtain the binding isotherms. Although the heat released due to dilution is smaller than the heat released due to binding, it is still of the same order of magnitude. The heat of dilution changes with the purity of chloroform, especially it is sensitive to traces of water. Although care was taken to use chloroform of the same purity for the ITC measurements and the preparation of the ITO dispersions, still the purity might differ slightly from batch to batch. Although this will not change the generic behaviour of the ITC data, still it increases the signal to noise ratio and increases the error of the fit. The reason of the endothermic contribution to the heat signal at the highest ITO concentration (10 mM ITO molecules) needs to be resolved in future experiments.

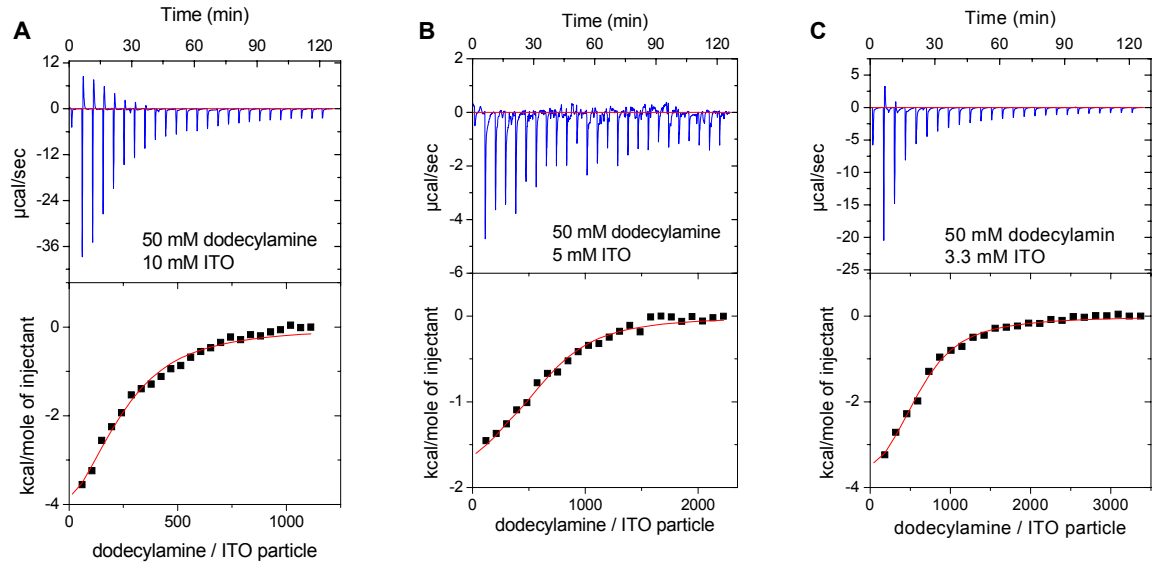

Fig S7. Top panels**:** Twenty four injections of 1.5µl dodecylamine in chloroform were titrated into a cell containing ITO nanoparticles dispersed in chloroform, varying the concentration of ITO while keeping the concentration of dodecylamine constant, 50 mM. A) 10 mM ITO molecules, B) 5 mM ITO molecules, C) 3.3 mM ITO molecules. The bottom panels give the binding isotherms. The solid red line shows the fit of the data points using a one site model.[S5,S6]

Varying the concentration of amine per injection does not change the shape of the heat curves. Again, the absolute values differ, i.e. $\Delta H = (-13 \pm 7)$ kJ/mol. The ITC curve of the lowest concentration of dodecylamine is hardly significant, because of the poor signal to noise ratio, Fig. S8A, caused by the low binding constant [$K \approx (0.5 \cdot 10^4\ \text{mol}^{-1}\ \ldots 4 \cdot 10^4)\ \text{mol}^{-1}$] and low ligand concentration.[S5,S6] It is unclear why this measurement shows a lower stoichiometry factor ($N < 50$) compared to the measurements at higher concentration of dodecylamine.

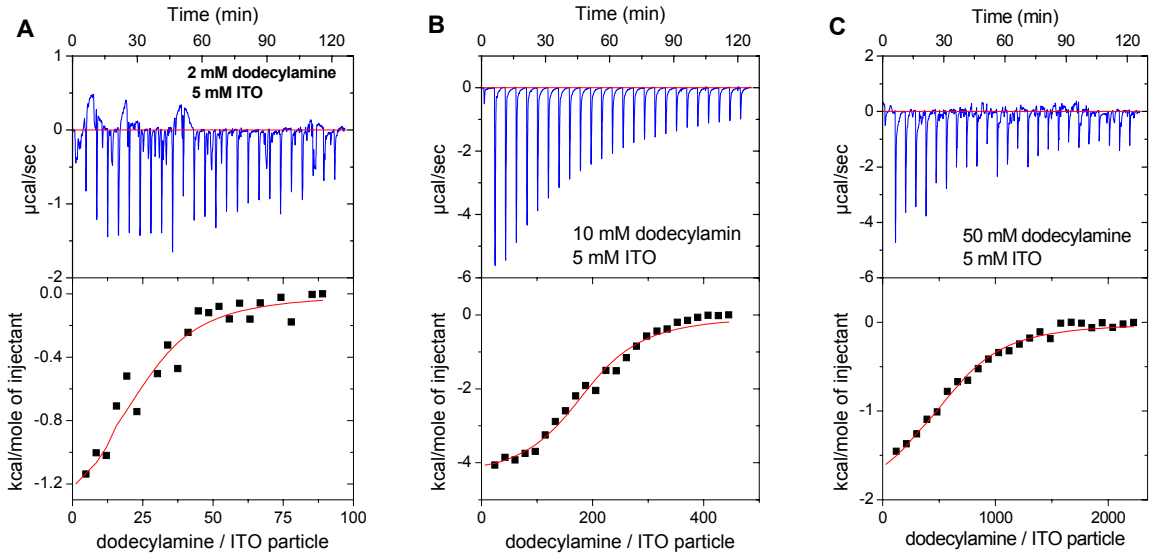

Fig S8. Top panels**:** Twenty four injections of 1.5µl dodecylamine in chloroform were titrated into ITO solutions, varying the concentration of dodecylamine while keeping the concentration of ITO constant, 5 mM ITO molecules. A) 2 mM dodecylamine, B) 10 mM dodecylamine, C) 50 mM dodecylamine. The bottom panels give the binding isotherms. The solid red line shows the best fit of the data points using a one site model.[S5,S6]

For interpretation of the ITC curves, it needs to be taken into consideration that the amines are added to agglomerated particles. The deagglomeration will cause heat changes that can be large or small

compared to the heat released by the binding of the stabilisers. It is conceptually impossible to perform this measurement using isolated unstabilised particles. However, it is known from theoretical calculations that the interaction potential of small nanoparticles is much lower than for larger colloidal particles. For example, the interaction potential of ZnO nanoparticles has been recently shown to be in the range of less than 1 kT (see [S7]), which amounts to < 2.5 kJ mol^{-1}. Assuming that the systems are rather similar, with the measured thermodynamic values varying between -21 kJ mol^{-1} and +17 kJ mol^{-1}, we can infer that the binding of the stabiliser dominates the heat changes, with the contributions of the deagglomeration process being almost an order of magnitude smaller. Also, the contribution of the deagglomeration process can be expected as rather similar for all systems, and thus would not have any influence on the observed trend for different stabilisers.

Still, we tested whether the ITC curve of stabilised and unstabilised particles resemble, Fig. S9. The heat changes associated with the titration of dodecylamine dissolved in chloroform (50 mM) into unstabilised ITO nanoparticles dispersed in $CHCl_3$ are shown in Fig. S9A, blue curve. Without changing the sample material, we performed a second titration measurement. We took the stabilised dispersion and titrated dodecylamine dissolved in chloroform (50 mM) into it. Now, the heat changes (Fig. S9A, black curve) resembled those of the dilution measurement, Fig. S9A, red curve. Therefore, no further binding of the additional amine to the stabilised particles can be detected. After waiting for 24 h, we repeated the measurement a second time, i.e. dodecylamine dissolved in chloroform was titrated into the already (twice) stabilised dispersions of ITO nanoparticles in $CHCl_3$, green curve in Fig. S5B. The heat signals fall below those of the dilution curve, supporting that the titrated amine does not bind to the surface of the particles. The heat even falls below those of the dilution because chloroform is already partially saturated with amine.

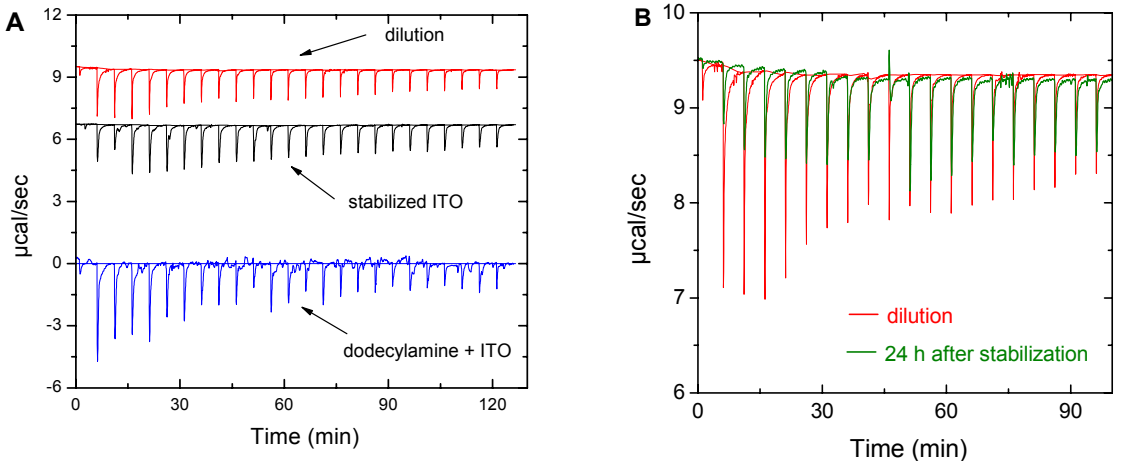

Fig S9. 24 injections of 50 mM dodecylamine dissolved in chloroform were added to 5 mM ITO nanoparticles dissolved in chloroform (blue line in Fig. S8A). The measurement was repeated after 1.5 h (black line in Fig. S8A), and 24 h (green line in Fig. S8B). The successive measurements were done without changing sample material. In case of the dilution measurement (red line in Fig. S8B), dodecylamine dissolved in chloroform was added to chloroform. Injecting dodecylamine to the stabilised ITO particles gave rise to heat changes that resemble those of the dilution measurement, (green line in Fig. S8B).

References

S1 J. Ba, D. F. Rohlfing, A. Feldhoff, T. Brezesinski, I. Djerdj, M. Wark and M. Niederberger, *Chem. Mater.*, 2006, **18**, 2848.
S2 D. I. Svergun, *J. Appl. Crystallogr.* 1992, **25**, 495.
S3 (*a*) J. G. Wu, J. Y. Li, G. Y. Li, D. G. Long, R. M. Weis, *Biochemistry*, 1996, **35**, 4984;
(*b*) L. Garciafuentes, P. Reche, O. Lopezmayorga, D. V. Santi, D. Gonzalezpacanowska, C. Baron, *Eur. J. Biochem.*, 1995, **232**, 641;
(*c*) X. G. Qu, J. S. Ren, P. V. Riccelli, A. S. Benight, J. B. Chaires, *Biochemistry*, 2003, **42**, 11960;
(*d*) J. R. Livingstone, *Nature*, 1996, **384**, 491.
S4 I. Jelesarov, H. R. J. Bosshard, *Mol. Recognit.*, 1999, **12**, 3.
S5 L. Indyk, H. F. Fisher, *Methods Enzymol.*, 1998, **295**, 350.
S6 T. Wiseman, S. Williston, J. F. Brandts, L. N. Lin, *Anal. Biochem.*, 1989, **179**, 131.
S7 D. Segets, R. Marczak, S. Schäfer, C. Paula, J.-F. Gnichwitz, A. Hirsch, W. Peukert, *ACS Nano*, 2011, **5**, 4658.